Electrochemical Model Based Fault Diagnosis of a Lithium Ion Battery using Multiple Model Adaptive Estimation Approach

Md Ashiqur Rahman
Mechatronics Research Lab
Purdue School of Engineering and Technology, IUPUI
rahman2@iupui.edu

Sohel Anwar, *Member*, *ASME*
soanwar@iupui.edu
Afshin Izadian, *Senior Member*, *IEEE*
aizadian@iupui.edu

Abstract— In this paper, we present an innovative approach in detecting fault conditions in a battery in which multiple model adaptive estimation (MMAE) technique is applied using electrochemical model of a Li-Ion cell. This physics based model of Li-ion battery (with $LiCoO_2$ cathode chemistry) with healthy battery parameters was considered as the reference model. Battery fault conditions such as aging, overcharge, and over discharge cause significant variations of parameters from nominal values and can be considered as separate models. Output error injection based partial differential algebraic equation (PDAE) observers are used to generate the residual voltage signals. These residuals are then used in MMAE algorithm to detect the ongoing fault conditions of the battery. Simulation results show that the fault conditions can be detected and identified accurately which indicates the effectiveness of the proposed battery fault detection method.

***Keywords*— Electrochemical model, Fault detection, Lithium-Ion batteries, MMAE, PDAE observer.**

NOMENCLATURE

c_e	Lithium ion concentration in the electrolyte phase
c_s	Lithium ion concentration in the active materials in both electrodes
$\bar{c}_{s,i}$	Volume-averaged concentration of a single particle
D_e	Diffusivity at electrolyte phase
D_s	Diffusivity at solid phase
$f_{c/a}$	Mean molar activity coefficient
F	Faraday constant
i_e	Current in the electrolyte phase
i_0	Exchange current density
I	Load current
J_n	Molar ion fluxes between the active materials in electrodes and the electrolyte
L^-	Length of negative electrode
L^+	Length of positive electrode
n	Number of active materials
R	Universal gas constant
R_P	Radius of the spherical particles
t_c^0	Transference number
T	Average internal temperature
U	Open circuit potential
V	Cell voltage
α_a	Charge transfer coefficient in anode
α_c	Charge transfer coefficient in cathode
γ	Observer gain constant
φ_e	Potential at electrolyte phase
φ_s	Potential at solid phase
ε_e	Volume fraction at electrolyte phase
ε_s	Volume fraction at solid phase
η	Over-potential for the reactions
ρ^{avg}	Average density
κ	Rate constant for the electrochemical reaction

INTRODUCTION

Li-Ion rechargeable batteries are one of the major power sources which are being thought of as the future energy sources in many sectors including automotive and communication sectors. Lithium Ion batteries are already in use in these areas, specifically in hybrid electric vehicles (HEV) as well as electric vehicles (EV) along with major portable electronic devices. In the past few years, usage of Li-Ion battery has remarkably increased due to the advantageous features as compared to other types of rechargeable batteries, namely the higher energy to weight ratio, lowest memory effects, lower self-discharge rates, and comparatively lower overall cost [2]. To ensure the optimal operation of Li-Ion battery without sacrificing the stated features, fault condition monitoring is of critical importance. These fault conditions can cause serious negative impact on the battery operation and life if they are not detected and managed quickly.

Based on the usage of the battery and type of operations involved, a number of fault detection and diagnosis (FDD) methodologies have been developed. All the model based FDD techniques make use of two major types of model, namely the equivalent circuit based models and true physics based models. In equivalent circuit based models, the battery is modeled by assuming that the true behavior of the battery is attainable using a combination of voltage source, capacitors, resistors, and Warburg impedances. The circuit parameters of the stated components are experimentally determined, in which the insight into the real physics of the battery is

ignored. This approach does not deal with the real dynamics of the battery chemistry.

On the other hand, the real physics based models, such as the one presented by Doyle, Fuller, and Newman [3] are primarily based on partial differential equations which contains all the required information regarding the true battery chemistry. This electrochemical model is based on the concentrated solution theory [4]. However this model is too complex to be used in a real time application. Model reduction via realistic simplifying assumption is used to overcome this issue. The work presented in this paper is based on the reduced order partial differential equation [5] representing the electrochemical battery model.

A large body of work exists that aims at the fault detection and diagnosis of rechargeable batteries. Adaptive estimation technique has been used in [6], which is based on equivalent circuit model. Extended Kalman filter (EKF) was utilized to estimate the state variables of the non-linear battery model that was used in this paper. EKF is based on an approximation of Taylor series, which cannot deal with highly non-linear systems. Another shortcoming of this work is that, it did not consider one of the major variable in the battery system, i.e. temperature. An adaptive recurrent neural network (ARNN) for prediction of remaining useful life (RUL) was used in [7], which is also modeled based on equivalent circuits. Synthesized design of Luenberger observer (LO) was adopted in [8] along with equivalent circuit model for fault isolation and estimation. The used observer works well with minimum or no measurement noise in the system. But this methodology does not perform well when significant measurement nose is present in the system.

Other major studies related to state of health (SOH) and remaining useful life (RUL) of Li Ion battery is based on data-driven methods. In [9], the data-driven method is presented on the diagnosis and prognosis of the battery health in an alternative powertrain. For estimation purposes, the authors used a support vector machine (SVM) type machine learning technique. A similar methodology is adopted a conditional three-parameter capacity degradation model in [10]. Kozlowski [11] presented a battery parameter identification, estimation and prognosis methodology presented using several techniques, e.g. neural network (NN), auto regressive moving average (ARMA), fuzzy logic (FL) and impedance spectroscopy (IS) etc. Since the data-driven method is based on the relationship between input and output, the real physics of the battery model is ignored in this approach as is in ECM.

Multiple model adaptive estimation (MMAE) is used in this work to detect the faults in a Li-ion battery. This adaptive estimation method requires representation of different fault scenarios, generate the residual signals and then to isolate the faults of different kinds using the algorithm. The generation of residuals and evaluation of them plays a vital role on the performance of the diagnosis [12]. In this work, the residuals are generated by comparing the simulated outputs of the fault models with the simulated output of the true plant model.

The work presented here aims at detecting several faults, i.e. aging, over-discharge (OD), and over-charge (OC) along with the detection of the healthy model. Among the stated fault scenarios in a Li-ion battery, OD and OC are critical for maintaining the health of the battery. While over-charging can lead to overheating that can lead to the vaporization of active material and explosion, over-discharge can short circuit the battery cell [13]. However, if these faults can be detected quickly according to the described methodology, steps can be taken to solve the issues before the faults can go to their extreme conditions.

ELECTROCHEMICAL BATTERY MODEL

The electrochemical battery model captures the spatiotemporal dynamics of Li-ion concentration, electrode potential in each phase and the Butler-Volmer kinetics which governs the intercalation reactions. A schematic of the model is provided in Fig. 1.

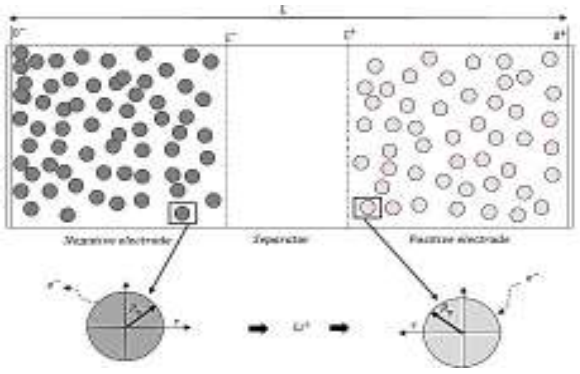

Fig. 1: Schematic Li-ion battery geometry [1].

From the above geometry, it is clear that, the considered geometry considers the dynamics of Li-ion cell only in X-direction. So, our model is a 1-D spatial model where variations of the dynamics in Y and Z directions in not considered. Another assumption here is that, Li-ion particles are considered to be composed of spherical shape with mean radius of $R_p$everywhere along X-axis[14].

Fig.1 shows the main regions of the Li-ion battery model. The entire spatial length is divided into three regions, namely, negative electrode (ranges from 0^- to L^-), separator (ranges from L^- to L^+) and the positive electrode (ranges from 0^+ to L^+). Two electrodes are separated by the thin and porous separator region through which only lithium ions (Li^+) can be passed, i.e. the current in the separator is carried away by the ions.

The involved state variables of the full battery model at any instantaneous time, t and distance, x are lithium ion concentration in the electrolyte phase $c_e(x,t)$, lithium ion

concentration in the active materials in both electrodes $c_s(x,r,t)$, potential at electrolyte phase $\varphi_e(x,t)$, potential at solid states $\varphi_s(x,t)$, current in the electrolyte phase $i_e(x,t)$, molar ion fluxes between the active materials in electrodes and the electrolyte $J_n(x,t)$ and the average internal temperature $T(t)$ [5].

The governing equations of the electrochemical model of the Li-ion battery are [3, 5, 14, 15] :

$$\varepsilon_e \frac{\partial c_e(x,t)}{\partial t} = \frac{\partial}{\partial x}\left(\varepsilon_e D_e \frac{\partial c_e(x,t)}{\partial x} + \frac{1-{t_c}^0}{F} i_e(x,t)\right) \quad (1)$$

$$\frac{\partial c_{s,i}(x,r,t)}{\partial t} = \frac{1}{r^2}\frac{\partial}{\partial r}\left(D_{s,i}\, r^2 \frac{\partial c_{s,i}(x,r,t)}{\partial r}\right) \quad (2)$$

$$\frac{\partial \phi_e(x,t)}{\partial x} = -\frac{i_e(x,t)}{\kappa} + \frac{2RT}{F}(1-{t_c}^0) \times \left(1 + \frac{d \ln f_{c/a}}{d \ln c_e(x,t)}\right)\frac{\partial \ln c_e(x,t)}{\partial x} \quad (3)$$

$$\frac{\partial \phi_s(x,t)}{\partial x} = \frac{i_e(x,t) - I(t)}{\sigma} \quad (4)$$

$$\frac{\partial i_e(x,t)}{\partial x} = \sum_{i=1}^{n} \frac{3\,\varepsilon_{s,i}}{R_{p,i}} F J_{n,i}(x,t) \quad (5)$$

$$J_{n,i}(x,t) = \frac{i_{0,i}(x,t)}{F}\left(e^{\frac{\alpha_a F \eta_i(x,t)}{RT}} - e^{\frac{-\alpha_c F \eta_i(x,t)}{RT}}\right) \quad (6)$$

Here $i_{0,i}(x,t)$ is the exchange current density and $\eta_i(x,t)$ is the over-potential for the reactions, equations of which are:

$$i_{0,i}(x,t) = r_{eff,i} c_e(x,t)^{\alpha_a} ({c_{s,i}}^{max} - c_{ss,i}(x,t))^{\alpha_c} c_{ss,i}(x,t)^{\alpha_c} \quad (7)$$

$$\eta_i(x,t) = \phi_s(x,t) - \phi_e(x,t) - U\left(c_{ss,i}(x,t)\right) - F R_{f,i} J_{n,i}(x,t) \quad (8)$$

Here $c_{ss,i}(x,t)$ is the i^{th} concentration at solid phase evaluated at r= $R_{p,i}$, $U\left(c_{ss,i}(x,t)\right)$ is the open circuit potential of the i^{th} active material in the solid phase and ${c_{s,i}}^{max}$ is the maximum possible concentration in the solid phase of the i^{th} active material and this is a constant[5].

$$\rho^{avg} c_p \frac{dT(t)}{dt} = h_{cell}\left(T_{amb}(t) - T(t)\right) + I(t)V(t) - \sum_{i=1}^{n}\left[\int_{0^-}^{0^+} \frac{3\,\varepsilon_{s,i}}{R_{p,i}} F J_{n,i}(x,t) \Delta U_i(x,t) dx\right] \quad (9)$$

Where,

$$\Delta U_i(x,t) \triangleq U_i(\bar{c}_{s,i}(x,t) - T(t)\frac{\partial U_i(\bar{c}_{s,i}(x,t))}{\partial T})$$

Here, $\bar{c}_{s,i}(x,t)$ is the volume-averaged concentration of a single particle, which is again defined as [5]

$$\bar{c}_{s,i}(x,t) \triangleq \frac{3}{{R_{p,i}}^3}\int_0^{R_{p,i}} r^2\, c_{s,i}(x,r,t)\, dr$$

In the above equations ε_e, $\varepsilon_{s,i}$, σ, R, $R_{p,i}$, F, α_a, α_c, c_p, ρ^{avg}, h_{cell} and ${t_c}^0$ are all constant parameters, κ, $f_{c/a}$ and D_e are dependent on electrolyte concentration and temperature and $r_{eff,i}$, $D_{s,i}$ and $R_{f,i}$ are Arrhenius-like parameters which follows the equation, $\theta(T) = \theta_{T_0}\, e^{A_\theta((T(t)-T_0)/T(t)T_0)}$.

Boundary conditions for the above model are $\frac{\partial c_e(0^-,t)}{\partial t} = 0$, $\frac{\partial c_e(0^+,t)}{\partial t} = 0, i_e(0^-,t) = 0$, $i_e(0^+,t) = 0$ and $\phi_e(0^+,t) = 0$.

Output of the model is, $V(t) = \Phi_s(0^+,t) - \Phi_s(0^-,t)$

Other few equations used during the simulation of the battery model are:

$$\theta_p = C_{s,p\ at\ r=Rp}/C_{s,p,max}$$

$$U_p = \frac{-4.656+88.669{\theta_p}^2-401.119{\theta_p}^4+342.909{\theta_p}^6-462.471{\theta_p}^8+433.434{\theta_p}^{10}}{-1+18.933{\theta_p}^2-79.532{\theta_p}^4+37.311{\theta_p}^6-73.083{\theta_p}^8+95.96{\theta_p}^{10}} \quad (10)$$

$$\theta_n = C_{s,n\ at\ r=Rn}/C_{s,n,max}$$

$$U_n = 0.7222 + 0.1387\theta_n + 0.029{\theta_n}^{0.5} - \frac{0.0172}{\theta_n} + \frac{0.0019}{{\theta_n}^{1.5}} + 0.2808\exp(0.90 - 15\theta_n) - 0.7984\exp(0.4465\theta_n - 0.4108) \quad (11)$$

MODEL REDUCTION AND PDAE OBSERVER EQUATIONS

Due to the complexity of the stated PDE model, the model is reduced based on few more assumptions. The model is intended to be reduced in such a way that, it will be a simple one from the simulation point of view by maintaining the ability to capture all the cell dynamics. The key assumption is the constant electrolyte concentration, i.e. $c_e(x,t) = c_e$ [5]. Another on is the introduction of an approximate solution of the diffusion equation in solid active materials presented in [16].

Using these two assumptions along with the boundary conditions, the reduced model equations:

$$\frac{\partial}{\partial t}\bar{c}_{s,i}{}^{\pm}(x,t) = -\frac{3}{R_i^{\pm}} J_{n,i}{}^{\pm}(x,t)$$

$$\frac{\partial}{\partial t}\bar{q}_{s,i}{}^{\pm}(x,t) = -\frac{30}{(R_i^{\pm})^2}\bar{q}_{s,i}{}^{\pm}(x,t) - \frac{45}{2(R_i^{\pm})^2} J_{n,i}{}^{\pm}(x,t)$$

$$c_{ss,i}{}^{\pm}(x,t) = \bar{c}_{s,i}{}^{\pm}(x,t) + \frac{8R_i^{\pm}}{35}\bar{q}_{s,i}{}^{\pm}(x,t) - \frac{R_i^{\pm}}{35 D_{s,i}{}^{\pm}} J_{n,i}{}^{\pm}(x,t)$$

$$J_{n,i}{}^{\pm}(x,t) = \frac{i_{0,i}{}^{\pm}(x,t)}{F}\left(e^{\frac{\alpha_a F \eta_i{}^{\pm}(x,t)}{RT}} - e^{\frac{-\alpha_c F \eta_i{}^{\pm}(x,t)}{RT}}\right)$$

$$\frac{\partial i_e{}^{\pm}(x,t)}{\partial x} = \sum_{i=1}^{n} \frac{3\,\varepsilon_{s,i}{}^{\pm}}{R_i^{\pm}} F J_{n,i}{}^{\pm}(x,t)$$

$$\frac{\partial \phi_s{}^{\pm}(x,t)}{\partial x} = \frac{i_e{}^{\pm}(x,t) - I(t)}{\sigma^{\pm}}$$

$$\frac{\partial \phi_e{}^{\pm}(x,t)}{\partial x} = -\frac{i_e{}^{\pm}(x,t)}{\kappa^{\pm}}$$

$$\rho^{avg} c_p \frac{dT(t)}{dt} = h_{cell}\left(T_{amb}(t) - T(t)\right) + I(t)V(t) - \sum_{i=1}^{n}\left[\int_{0^-}^{L^-} \frac{3\varepsilon_{s,i}{}^{-}}{R_{p,i}{}^{-}} F J_{n,i}{}^{-}(x,t) \Delta U_i{}^{-}(x,t) dx\right] - \sum_{i=1}^{n}\left[\int_{0^+}^{L^+} \frac{3\varepsilon_{s,i}{}^{+}}{R_{p,i}{}^{+}} F J_{n,i}{}^{+}(x,t) \Delta U_i{}^{+}(x,t) dx\right]$$

During the design of this PDAE observer, there was introduced a feedback of error between the measured outputs and the calculated outputs [5]. This feedback was maintained in such a way that all the variables being estimated converges to their true values [17]. The PDAE observer gain are linear corrective terms via output injection only for the

volume averaged concentrations in the individual electrodes and the internal average temperature [5]. The gain values were determined by trial and error method during the simulation for which the error value is the minimum one.

The PDAE observer equations are the followings:

$$\frac{\partial}{\partial t}\hat{c}_{s,i}^{\pm}(x,t) = -\frac{3}{R_i^{\pm}}\hat{J}_{n,i}^{\pm}(x,t)+\gamma_i^{\pm}(V(t)-\hat{V}(t))$$

$$\frac{\partial}{\partial t}\hat{\bar{q}}_{s,i}^{\pm}(x,t) = -\frac{30}{(R_i^{\pm})^2}\hat{\bar{q}}_{s,i}^{\pm}(x,t) - \frac{45}{2(R_i^{\pm})^2}\hat{J}_{n,i}^{\pm}(x,t)$$

$$\hat{c}_{ss,i}^{\pm}(x,t) = \hat{c}_{s,i}^{\pm}(x,t)+\frac{8R_i^{\pm}}{35}\hat{\bar{q}}_{s,i}^{\pm}(x,t) - \frac{R_i^{\pm}}{35D_{s,i}^{\pm}}\hat{J}_{n,i}^{\pm}(x,t)$$

$$\hat{J}_{n,i}^{\pm}(x,t) = \frac{\hat{\imath}_{0,i}^{\pm}(x,t)}{F}\left(e^{\frac{\alpha_a F\hat{\eta}_i^{\pm}(x,t)}{RT}} - e^{\frac{-\alpha_c F\hat{\eta}_i^{\pm}(x,t)}{RT}}\right)$$

$$\frac{\partial\hat{\imath}_e^{\pm}(x,t)}{\partial x} = \sum_{i=1}^{n}\frac{3\,\varepsilon_{s,i}^{\pm}}{R_i^{\pm}}F\hat{J}_{n,i}^{\pm}(x,t)$$

$$\frac{\partial\hat{\phi}_s^{\pm}(x,t)}{\partial x} = \frac{\hat{\imath}_e^{\pm}(x,t)-I(t)}{\sigma^{\pm}}$$

$$\frac{\partial\hat{\phi}_e^{\pm}(x,t)}{\partial x} = -\frac{\hat{\imath}_e^{\pm}(x,t)}{\kappa^{\pm}}$$

$$\rho^{avg}c_p\frac{d\hat{T}(t)}{dt} = h_{cell}\left(T_{amb}(t)-\hat{T}(t)\right)+I(t)\hat{V}(t)-$$
$$\sum_{i=1}^{n}\left[\int_{0^-}^{L^-}\frac{3\varepsilon_{s,i}^{-}}{R_{p,i}^{-}}FJ_{n,i}^{-}(x,t)\Delta U_i^{-}(x,t)dx\right]-$$
$$\sum_{i=1}^{n}[\int_{0^+}^{L^+}\frac{3\varepsilon_{s,i}^{+}}{R_{p,i}^{+}}FJ_{n,i}^{+}(x,t)\Delta U_i^{+}(x,t)dx]+\gamma_T^{\pm}(V(t)-\hat{V}(t)).$$

Observer output, $\hat{V}(t)=\hat{\phi}_s^{+}(0^+,t)-\hat{\phi}_s^{-}(0^-,t)$.

The equation of the observer gain in the two electrodes are given by $\begin{bmatrix}\gamma_i^{-}\\ \gamma_i^{+}\end{bmatrix} = \gamma\times\begin{bmatrix}\frac{1}{n^-\varepsilon_{s,i}{}^-L^-}\\ \frac{1}{n^+\varepsilon_{s,i}{}^+L^+}\end{bmatrix}$, where, n denotes number of active materials which is assumed one in our works.

MULTIPLE MODEL ADAPTIVE ESTIMATION (MMAE) TECHNIQUE

This adaptive estimation technique which is a special type of fault detection method is adopted in our work with the electrochemical model of Li-ion battery. In this estimation (MMAE) technique [18-22], as shown in Fig.2, various models run simultaneously while all the models are excited by the same input signal. MMAE in this work uses PDAE observer outputs of different models (coming from due to parameter variations). If there are total "n" models, there will be (n-1) outputs represents the faults or unhealthy scenarios [6], the remaining one is the actual plant model.

The distinguishing feature of MMAE technique is that, it provides a scope of fault detection based on possible fault scenarios along with the actual model. Main advantage of using MMAE as compared with other possible ways of fault detection (fuzzy logic, SVM etc.) is that, it provides a probabilistic approach of condition monitoring [6] based on the differences of outputs between the actual model and all other individual fault models which is more reliable in case of fault detection.

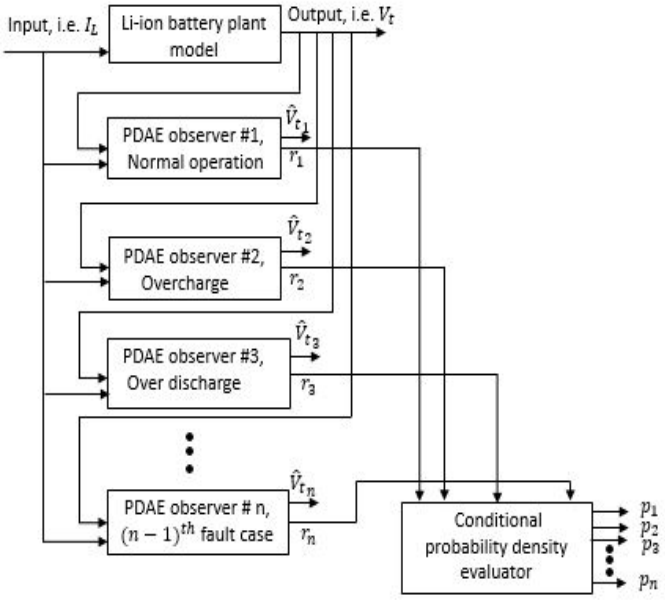

Fig.2.Residual and probability generation from multiple models

Here, $p_1 + p_2+p_3+\ldots\ldots+p_n = 1$

The conditional probabilities require a *priori* samples to compute the current values and are normalized over a complete sum of conditional probabilities of all systems. The probability for the n^{th} model at time sample k is given by [6, 20-22]

$$p_{n,k} = \frac{f_{z(k)|a,Z(k-1)}(z_k|a_n,Z_{k-1})p_n(k-1)}{\sum_{j=1}^{n}f_{z(k)|a,Z(k-1)}(z_k|a_j,Z_{k-1})p_j(k-1)}$$

Where, $f_{z(k)|a,Z(k-1)}(z_k|a_n,Z_{k-1})p_n(k-1)$ is the conditional probability density function of the n^{th} model considering the history of the measurements.

The conditional probability function is expressed as [20-22]:

$f_{z(k)|a,Z(k-1)}(z_k|a_n,Z_{k-1}) = \beta_n\exp(\circ)$

Where,$\beta_n = \frac{1}{(2\pi)^{l/2}|\psi_n(k)|^{1/2}}$

Where, l is the measurement dimension and equal to 1 and $(\circ) = \frac{1}{2}\,r_{n,k}{}^T\psi_{n,k}{}^{-1}r_{n,k}$

Where, $r_{n,k}$ is the residual signal for the n^{th} model at time sample k. When the output of any of the available models matches with the output of the actual model which

simultaneously make the mean value of that residual signal to zero and the covariance of that particular signal is given [20-22] by,

$$\psi_{n,k} = C_{n,k} P_{n,k|k} {C_{n,k}}^T + R$$

Where $C_{n,k}$ is the output vector for n^{th} system at any time sample k. Moreover, $P_{n,k|k}$ represents the state covariance matrix while R is covariance matrix of measurement noise. We have used System Identification Toolbox in MATLAB to have P matrices for all the scenarios. We have taken the input current profile and the output voltage profile for all considered models in this procedure. We have considered a constant value of measurement noise covariance matrix R, which is actually 1×10^{-6}.

Using all possible residuals the conditional probabilities are evaluated. The largest conditional probability among all may be used as an indication of ongoing fault condition related to the involved specific residual[6].

SIMULATION & RESULTS

The parameters adopted for the simulation of the reduced electrochemical model is are given in the following table [23]:

Symbol	*Unit*	*Positive electrode*	*Separator*	*Negative electrode*
σ_i	S/m	100		100
$\varepsilon_{f,i}$		0.025		0.0326
ε_i		0.385	0.724	0.485
$c_{s,i,max}$	mol/m^3	51554		30555
$c_{s,i0}$	mol/m^3	0.4955×51554		0.8551×30555
c_0	mol/m^3		1000	
R_P	m	2.0×10^{-6}		2.0×10^{-6}
L_i	m	80×10^{-6}	25×10^{-6}	88×10^{-6}
R_{SEI}	Ωm^2			0.0
F	C/mol		96487	
R	$J/(mol\,K)$		8.314	
T	K		298.15	

Table 1. Electrochemical model parameters for $LiCoO_2$ cathode chemistry

Using all the parameters the actual model was formulated. Then this model was run under constant current density conditions, i.e. $30A/m^2$ & $15A/m^2$ discharge. The prior one denotes the C-rate while the later one indicates the discharge with C/2-rate. This part of simulation was performed to check the consistency of our model behavior with the theoretical characteristics of the battery system. The obtained results are shown in the following figure:

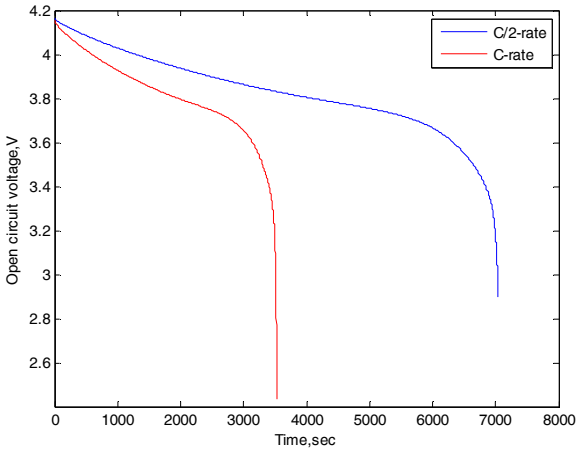

Fig.3. Open circuit voltage of Li-ion battery

From Fig.3, it is clear that, the battery is being discharged in near 1-hr in C-rate discharge while the time is near 2-hrs for C/2-rate discharge. So, it can be said that, the reduced model is designed well enough mainlining the consistency with the basic battery performance criteria. Later on, this model was observed with the PDAE observer for the use of fault detection.

After obtaining a well-designed model, we have gone through the fault detection of this battery system. For this purpose a sinusoidal current profile was selected as the input to the battery model. Fig.4 demonstrates the input current profile:

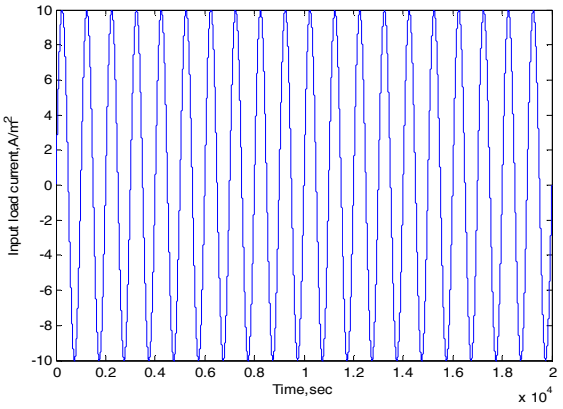

Fig.4. Input load current profile

For this input signal, the PDAE observer for electrochemical battery model was verified. We have recorded the voltage response of the actual model and the observer voltage response with different values of the linear corrective terms. Trial and error method was adopted to finalize the value of PDAE observer gain, γ. Fig.5 represents the voltage response of both the actual model and also the observed model. For this input, obtained maximum cell voltage is 4.173V while the minimum is 4.135V.

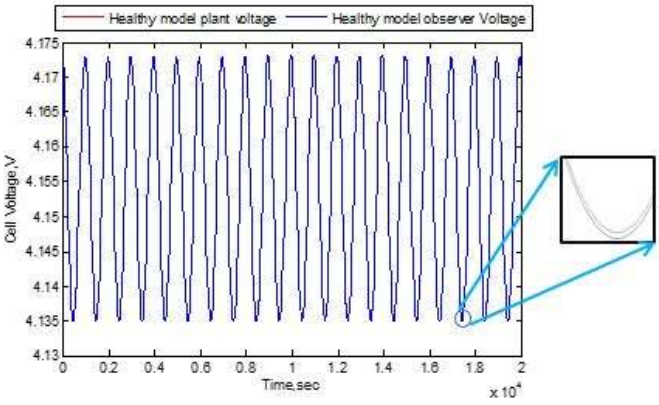

Fig.5. Healthy model plant and observed voltage response

The response in Fig.5 was obtained when $\gamma = 51 \times 10^{-3}$. From the response above, it is evident that, the observer is able to track the actual model with highest possible accuracy. Here the residual values are almost zero throughout the simulation. From this γ value, one can easily check the individual γ values in each electrode for having the best possible response by using the observer gain equation which is given in the modeling section of this paper.

Multiple models during the fault detection algorithm was yielded due to the parameter variations from model to model. Table 2 summarizes the considered changes in parameters. It is clear from the table that, there exists substantial changes in parameter values when compared with the actual model.

Parameter	*Healthy*	*Aged*	*OD*	*OC*
$D_n(m^2/s)$	3.9×10^{-14}	4.875×10^{-15}	7.8×10^{-15}	6.5×10^{-15}
$D_p(m^2/s)$	1.0×10^{-14}	1.5×10^{-14}	5.0×10^{-15}	5.0×10^{-15}
$k_n(mol/(sm^2)/(mol/m^3))$	5.0307×10^{-11}	6.2884×10^{-12}	1.0061×10^{-11}	8.38×10^{-12}
$k_p(mol/(sm^2)/(mol/m^3))$	2.334×10^{-11}	2.33×10^{-11}	1.17×10^{-11}	1.17×10^{-11}

Table 2. Parameter variations during model building

The voltage response of overall plant model due to the four scenarios for same input signal is given in Fig.6. First & last 4k samples in overall plant is from healthy model, next 4k is from aged model, next 4k samples are due to over discharge model and the next 4k samples are from overcharge model. Maximum value of the plant model for the given input is 4.184 V while the minimum is 4.124 V.

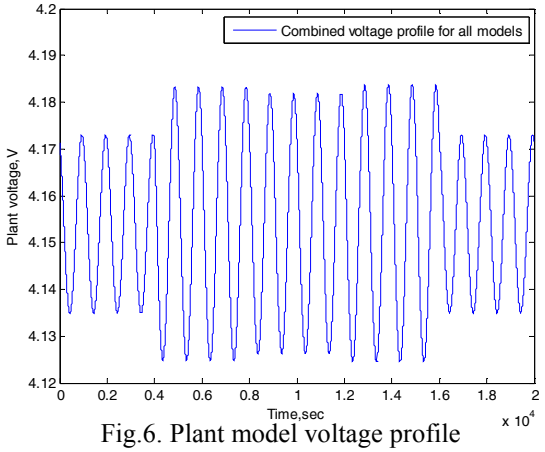

Fig.6. Plant model voltage profile

To determine the effectiveness of this fault detection approach, the above described parameter variations represents the fault cases to be detected. Overall simulation was run for total 20k samples among which the first and last 4k samples were simulated for the healthy condition.

Overall simulation time was divided equally into five parts which occurs as following consecutively[6]:

1. For the first 4k samples are healthy cell operation
2. For next 4k samples Aged fault condition
3. For next 4k samples OD fault condition
4. For next 4k samples OC fault condition
5. For last 4k samples, the battery is back into the healthy condition

Whenever the residual values for any of the fault scenarios goes to zero, it indicates that the output for this case matches with the actual model and the probability of occurring this case is higher as compared to others. Fig.7 represents the residual values for all of the given scenarios.

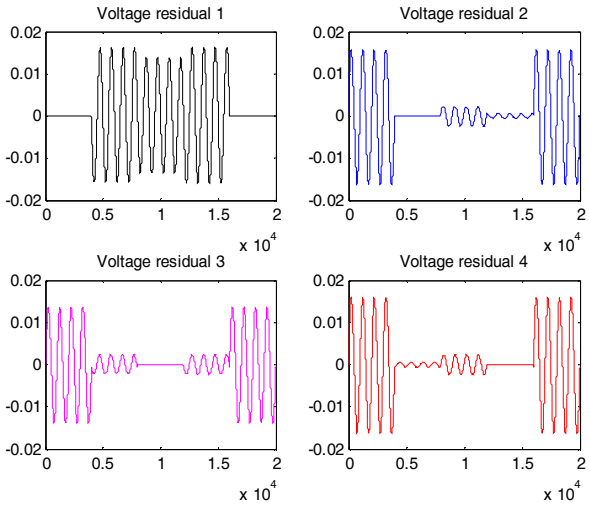

Fig.7. Voltage residuals for considered cases

From the above residual plot, it is clear that, the residuals are following the order we created for the fault scenarios. Later on, we used this residuals for finding the conditional probabilities for each fault scenarios.

During this fault detection, it is also assumed that, at any instance there can occur only one fault case among the five assumed scenarios. The indication of fault occurring comes from conditional probability evaluation. Whenever the value of the conditional probability for any of the faults goes to 1 keeping the probability of others in 0, then at that instance that fault is the responsible one.

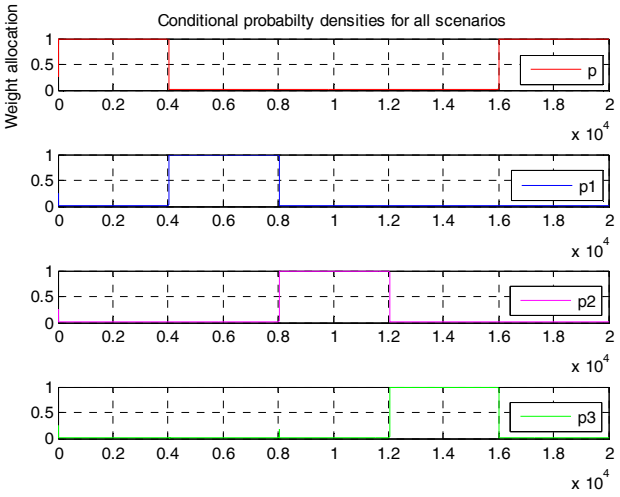

Fig.8. Conditional probability density for four scenarios

In Fig.8 p, p1, p2 & p3 represents the probability of occurring the healthy, aged, OD & OC scenarios respectively. If we look at the plot, it is clear that, during first and last 4k samples, healthy battery condition prevails as expected, i.e. probability is 1 while the probability of occurring any other faults are at 0. In next 4k samples, the probability of the aged condition is 1 while the probability of other situations are 0. This indicates that, the aged fault case is detected for this samples which higher accuracy. Similar situation is true also for OD and OC fault cases. This detected probabilities can be used in real time for the fault diagnosis. Probabilities of occurring different faults from this electrochemical model is obtained as expected using MMAE technique.

CONCLUSION

This paper incorporated MMAE algorithm for fault detection from electrochemical model of lithium ion battery. A linear corrective term was introduced while using the PDAE observer along with the reduced electrochemical model. Apart from the healthy (original) model, three major fault scenarios (Aging, Over discharge & Over charge) were created. Simulation results show that, the MMAE technique is capable of detecting the presumed fault conditions with higher accuracy. Therefore this proposed methodology of fault detection based on electrochemical model using MMAE can be used in real time fault detection and can be further implemented for Li-ion battery fault diagnosis.

REFERENCES

[1] Smith KA, Rahn CD, Wang C-Y. Energy Conversion and Management 2007;48:2565.

[2] Chaturvedi NA, Klein R, Christensen J, Ahmed J, Kojic A. Modeling, estimation, and control challenges for lithium-ion batteries. American Control Conference (ACC), 2010: IEEE, 2010. p.1997.

[3] Doyle M, Fuller TF, Newman J. Journal of the Electrochemical Society 1993;140:1526.

[4] Newman J, Tiedemann W. AIChE Journal 1975;21:25.

[5] Klein R, Chaturvedi NA, Christensen J, Ahmed J, Findeisen R, Kojic A. 2012.

[6] Singh A, Izadian A, Anwar S. Fault diagnosis of Li-Ion batteries using multiple-model adaptive estimation. Industrial Electronics Society, IECON 2013-39th Annual Conference of the IEEE: IEEE, 2013. p.3524.

[7] Liu J, Saxena A, Goebel K, Saha B, Wang W. An adaptive recurrent neural network for remaining useful life prediction of lithium-ion batteries. DTIC Document, 2010.

[8] Chen W, Chen W-T, Saif M, Li M-F, Wu H. IEEE TRANSACTIONS ON CONTROL SYSTEMS TECHNOLOGY 2014;22:290.

[9] Nuhic A, Terzimehic T, Soczka-Guth T, Buchholz M, Dietmayer K. Journal of Power Sources 2013;239:680.

[10] Wang D, Miao Q, Pecht M. Journal of Power Sources 2013;239:253.

[11] Kozlowski JD. Electrochemical cell prognostics using online impedance measurements and model-based data fusion techniques. Aerospace Conference, 2003. Proceedings. 2003 IEEE, vol. 7: IEEE, 2003. p.3257.

[12] Ding SX. Model-based fault diagnosis techniques: Springer, 2008.

[13] Lee Y-S, Cheng M-W. Industrial Electronics, IEEE Transactions on 2005;52:1297.

[14] Chaturvedi NA, Klein R, Christensen J, Ahmed J, Kojic A. Control Systems, IEEE 2010;30:49.

[15] Albertus P, Christensen J, Newman J. Journal of the Electrochemical Society 2009;156:A606.

[16] Subramanian VR, Diwakar VD, Tapriyal D. Journal of The Electrochemical Society 2005;152:A2002.

[17] Klein R, Chaturvedi NA, Christensen J, Ahmed J, Findeisen R, Kojic A. State estimation of a reduced electrochemical model of a lithium-ion battery. American Control Conference (ACC), 2010: IEEE, 2010. p.6618.

[18] Izadian A, Famouri P. Control Systems Technology, IEEE Transactions on 2010;18:1233.

[19] Izadian A, Khayyer P, Famouri P. Industrial Electronics, IEEE Transactions on 2009;56:973.

[20] Hanlon PD, Maybeck PS. Aerospace and Electronic Systems, IEEE Transactions on 2000;36:393.
[21] Eide P, Maybeck P. Implementation and demonstration of a multiple model adaptive estimation failure detection system for the F-16. Decision and Control, 1995., Proceedings of the 34th IEEE Conference on, vol. 2: IEEE, 1995. p.1873.
[22] Eide P, Maybeck P. Aerospace and Electronic Systems, IEEE Transactions on 1996;32:1125.
[23] Subramanian VR, Boovaragavan V, Ramadesigan V, Arabandi M. Journal of The Electrochemical Society 2009;156:A260.